Calibration and 3D Measurement of Bionic Compound-eye Vision System

Hongmin Zhou [*1], Yuan Li [*1]

[*1]Beijing Institute of Technology, No. 5 Zhongguancun South Street
E-mail: 3120200993@bit.edu.cn, liyuan@bit.edu.cn

Abstract. In computer vision, the emerging large requirements on large field of view, small size and high sensitivity of interested objects, makes the research on artificial bionic compound eyes a new hot spot. On the basis of previous research, this paper designs and calibrates a compound eye system based on neural network model. The model and calibration can replace tedious developments with intelligent learning, the neural network model parameter identification. The experiments on 3D measurement of close-range objects verified the proposed method.

Keywords: Compound-eye, Neural network, Calibration, 3D measurement

1. INTRODUCTION

Nowadays, binocular vision, which is basically mature in related theories, is widely used in three-dimensional vision measurement. However, binocular vision is limited by its own hardware system, and is suitable for measuring objects of limited size or field of view environment. Therefore, while measuring large-size objects and targets in a large field of view, the equipment needs to meet the requirements of small volume, strong real-time and low cost. The biomimetic compound eye vision system can take advantage of the condition that the target object is imaged differently in different sub-eye channels to achieve three-dimensional measurement without adding components. Moreover, the compound eye vision system has the potential ability to archive large field of view, by adapting the configuration of panorama, which is of great research significance.

In 2000, Japanese scientist Tanida J led a research team to develop a flat compound eye TOMBO[1-3], which can reconstruct high-resolution images from low-resolution images. The research from the University of California, Berkeley proposes a curved microlens array similar in size to actual insects[4, 5]. The papers[6-11] are all attempts to resolve the contradiction between the flat image sensor and the curved micro-lens array. Researchers from Duke University have successfully developed Aware2[12], a compound-eye camera with a giga-pixel wide field of view. The research[13] shows a multi-focus sub-eye lens, which solves the problem of traditional compound eye structure that limits the acquisition of image information due to the single focal length of the lens.

The biomimetic compound eye vision system can take advantage of the condition that the target object is imaged differently in different sub-eye channels to achieve three-dimensional measurement without adding components, which is of great research significance. In this paper, based on previous studies on the design of the fly-eye system based on neural network model, eliminating the tedious development of complex calibration, a shift to the neural network model parameter identification, and measurement of three-dimensional close-range object.

2. THE DESIGN OF THE COMPOUND EYE SYSTEM

The compound eye system is mainly composed of hardware, image processing algorithms and neural network models. The working process of the system is as follows, the hardware system collects images in real time, the image processing program extracts and matches the feature points, and uses the feature points as input to obtain the stereo coordinates through the neural network.

This paper uses a planar compound eye structure, which consists of two parts: a camera and a microlens array. The micro-lens array is composed of 8*8 sub-eye lenses, and the sub-eyes are arranged horizontally and vertically and glued on a 12cm*12cm flat glass with optical glue, as shown in Fig 1(a), and each lens is outside. The diameter is 7.6mm and the focal length is 10mm. The camera is an ordinary camera with a resolution of 12 million pixels, and the distance between the camera and the lens array is 8cm. The principle of the compound eye structure is relatively simple. The microlens array images in different sub-eye lenses, and a single camera acts as a planar image sensor. A simple compound eye system can be obtained by combining the two. Its structure is shown in Fig 1(b) as shown.

3. IMAGE PROCESSING AND FEATURE EXTRACTION

After preprocessing the microlens array imaging obtained from the camera, sub-pixel-level corner points are extracted as feature points.

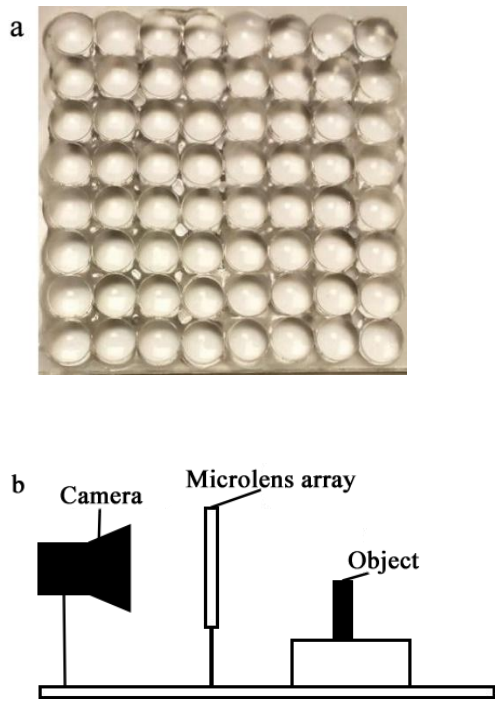

Fig. 1 Bionic compound eye hardware system: (a) Microlens physical image, (b) system structure.

How to effectively match the feature points after obtaining the feature points is one of the important factors affecting accuracy. The number of sub-eye channels in this project is 64. As the calculation amount of the compound-eye matching feature value increases exponentially with the increase of the number of sub-eye channels, the load of the system is increased, and the real-time performance of the system has been greatly affected. In order to enable the system to quickly and accurately locate the system, and according to the overlapping characteristics of the adjacent sub-eyes of the compound eye system, the grouped sub-eye channels are selected and the index table is established. First, number the sub-eyes, starting from the upper left corner, and gradually increasing from left to right, as shown in Fig 2(a); Second, each sub-eye and the surrounding four sub-eyes form a group, as shown in Fig 2(b), the number of adjacent sub-eyes in the sub-eye groups of the edges and corners are 3 and 2, respectively.

The entire search process is similar to searching and or counting. The central sub-eye of each group can be regarded as the parent node, and the adjacent child eye that has not been searched is the child node. Therefore, blind and heuristic search schemes can be used. Blind search is usually based on a predetermined search strategy, which is suitable for solving simple problems. Commonly used algorithms are: breadth first search, depth first search, bounded first search, etc.; heuristic search usually uses heuristic information to search, that is, information related to the problem, which can improve search efficiency.

This article draws on the breadth-first search strategy. The core idea of the breadth-first algorithm is, starting from the initial node, generate the first layer of nodes, check whether there are target nodes in these nodes, and if not, expand all nodes in the layer. Get the second-level node, and repeat the above steps, and expand in turn until the target node is found.

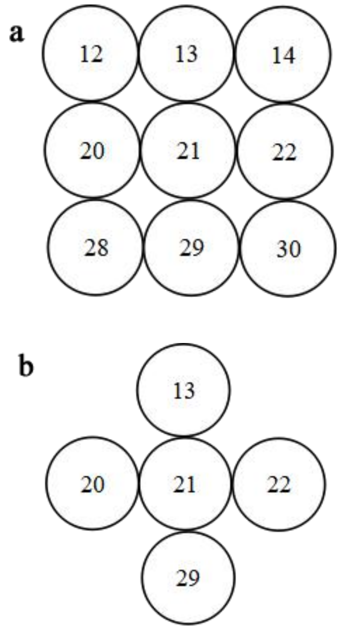

Fig. 2 Labeling and grouping of sub-eyes: (a) Part of the sub-eye number, (b) Example of sub-eye grouping

This article changes the breadth-first search strategy. The entire search process is as follows.

(1) First, establish a search flag table, each sub-eye corresponds to an element in the table and the initial value is 1, if a sub-eye has been searched, the corresponding element is set to zero;

(2) Starting from the sub-eye numbered 1, search for feature points in the direction of increasing number;

(3) If the search is not found, exit, return to (2), and start the search process for the next feature point; otherwise, use the breadth-first search strategy to search for the neighbors whose flag is 1 from the searched sub-eye Eye, only the condition for the end of the search is modified to that all the sub-eye nodes in this layer have not searched for the desired feature, and the search ends and starts to search for the next feature point.

4. IDENTIFICATION OF THE NEURAL NETWORK MODEL

The identification of the camera neural network model parameters is one of the two most important parts that affect the accuracy, because if its accuracy is poor, the output will be inaccurate no matter how accurate the feature coordinates extracted by image processing are. Since the number of compound eye sub-eyes is 64, the input data number of the neural network is 128, i.e., the two-dimensional point coordinates of the 64 sub-eyes, and the output is the three-dimensional coordinates in the world coordinate system. With repeated tests and experiments, it is found that there are many very similar input data, which are often only a few or dozens of pixels apart, and the normalization is more similar after the process, which leads to training errors. Therefore, based on the original input data, two more flags are introduced, the average of all input data and the square root of their sum of squares. The number of layers of the neural network model is selected as 4 layers, and the number of hidden layer nodes fully connected to the input layer is 20, the number of nodes in the other hidden layer is 10, the number of nodes in the input layer is 130, and the number of nodes in the output layer is 3.

The first step is to process the training data, using the image preprocessing algorithm, feature extraction algorithm and geometric target in section 2.2. Take the geometric target with a compound eye camera, extract and match the characteristic corner points in each sub-eye, and use these two-dimensional coordinates as the input of the neural network; select a world coordinate system arbitrarily to obtain the three-dimensional of each corner point in the world coordinate system The coordinates are used as the output set of training. Move the target along the horizontal, vertical, and vertical directions, and repeat the above steps to obtain enough training sets to make the results more accurate.

Because the inherent shortcomings of the traditional BP neural network may affect the accuracy and real-time performance of the system, this paper selects additional momentum items, dynamically adjusting the learning rate, and batch learning to optimize the BP neural network. The overall process is as follows:

(1) Process input and output data, normalize it, and initialize the weight;

(2) Input all the input data to calculate the error and weight adjustment, but the weight is not corrected, but accumulated;

(3) After completing the accumulation of all corrections and errors, first adjust the momentum coefficient and learning rate according to the changes at the time before and after the error, and then correct the weight;

(4) Finally, judge whether the error is less than the expected error or whether the number of learning times reaches the maximum number of learning times. If the judgment is true, push it out, otherwise return to step (2).

5. EXPERIMENTAL RESULT

5.1. Point Measurement Experiment

The experiment uses a right triangle as the target. Fig 3 is a test example. When extracting features, you can perform corner detection after preprocessing. Usually, three corners can be detected. Any corner can be connected to other corners to form a line. It can be determined by judging the angle between the two straight lines and the quadrant. To determine which is a right angle, Table 1 is the test result of the triangular target. Analyzing the experimental results, it can be seen that because the data for training the neural network is normalized, the accuracy of the smaller coordinates in the three-dimensional coordinates is lower than that of other coordinates.

Table. 1 Test result of right triangle target.

Number	Actual output /mm	Theoretical output /mm
1	(53.21 , 52.76 , 80.78)	(50.00 , 50.00 , 85.00)
2	(51.19 , 49.73 , 94.07)	(50.00 , 50.00 , 90.00)
3	(49.52 , 48.30 , 94.62)	(50.00 , 50.00 , 95.00)
4	(72.73 , 8.84 , 75.16)	(70.00 , 6.00 , 75.00)
5	(9.63 , 73.40 , 104.72)	(10.00 , 75.00 , 105.00)

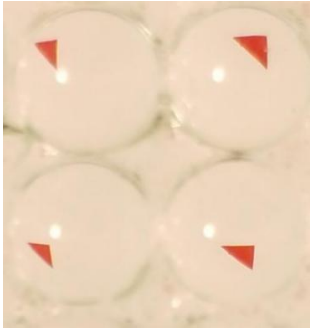

Fig. 3 Right triangle target imaging

5.2. Measurement Experiment of Flat Object

Passed the point measurement experiment, continue to test the compound eye system, this time is a test experiment on a flat object. Firstly, choose a rectangular parallelepiped with a size of $65mm \times 65mm \times 65mm$, and place the object at 95mm from the compound eye lens array. The compound eye imaging result of the measured object is shown in Fig 4(a). Secondly, the image is processed to extract the corner points corresponding to the vertices of the measured object, input into the neural network model, and the output results are shown in Table 2, and the modeling results are shown in Fig 4(b). Via the neural network operation, each of the side length of the compound eye system is measured cuboid: 64.977mm, 67.370mm, 66.960mm, 65.093mm, measurement error of less than 4%.

Table. 2 Cuboid test results.

Number	Actual output /mm	Theoretical output /mm
1	(7.88 , 69.07 , 94.85)	(7.90 , 69.00 , 95.00)
2	(72.85 , 69.18 , 94.99)	(72.9 , 69.00 , 95.00)
3	(7.88 , 1.70 , 94.87)	(7.90 , 4.00 , 95.00)
4	(72.97 , 2.22 , 95.00)	(72.90 , 4.00 , 95.00)

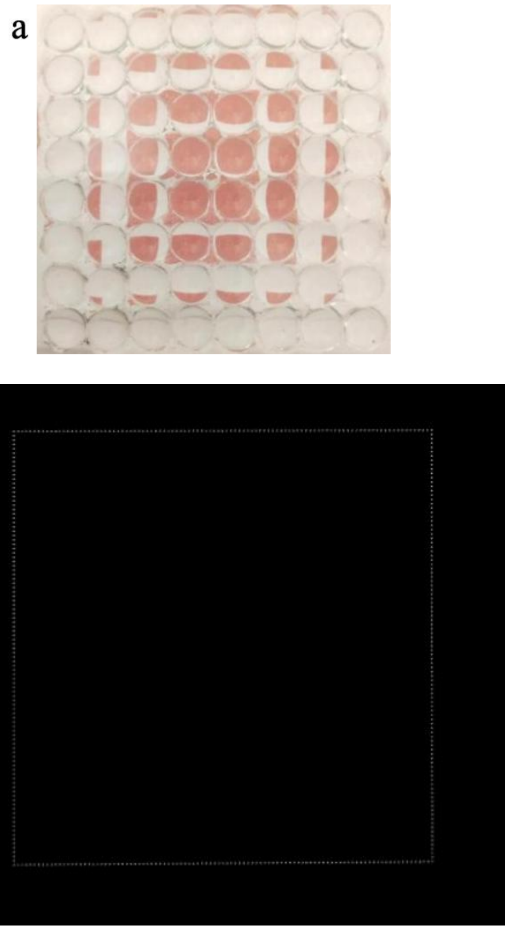

Fig. 4 Experimental results: (a) Compound eye imaging of flat objects, (b) Modeling results of flat objects

5.3. Stereo 3D Measurement Experiment

In order to further verify whether the compound eye system can accomplish three-dimensional measurements, the object in the plane test is placed obliquely. That is, the object is 105mm from the compound eye on the right side and 75mm from the compound eye on the left side. In this case, the compound eye system is used for measurement, the imaging is shown in Fig 5(a), and the modeling result is shown in Fig 5(b). Table 3 is the corner point measurement result, the length of each side is: 65.336mm, 64.681mm, 64.574mm, 64.605mm.

Table. 3 3D test results.

Number	Actual output /mm	Theoretical output /mm
1	(4.42 , 74.41 , 104.93)	(5.00 , 75.00 , 105.00)
2	(62.50 , 75.35 , 75.02)	(62.66 ,75.00 , 75.00)
3	(4.99 , 9.74 , 104.95)	(5.00 , 10.00 , 105.00)
4	(62.06 , 10.83 , 74.69)	(62.66 , 10.00 , 75.00)

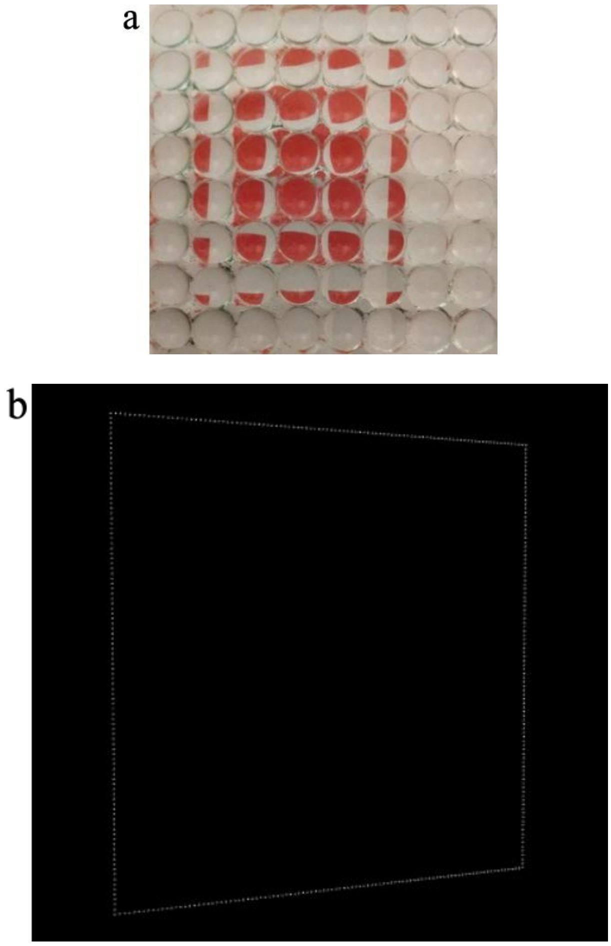

Fig. 5 Experimental results: (a) Compound eye imaging of flat objects, (b) 3D test modeling results

6. CONCLUSION

This paper proposes a mechanism for accelerating feature point matching and using neural network to fit the compound eye system model. The system can accurately model simple close-range objects. However, there are still shortcomings: lens distortion is serious; there is no isolation layer between the lenses, and mutual interference is serious. If these problems can be solved perfectly, more delicate objects can be measured.

REFERENCES:

[1] Tanida J, Yamada K. TOMBO: Thin observation module by bound optics[C]// Lasers and Electro-Optics Society, Leos the Meeting of the IEEE. IEEE,vol.1.2002:233-234.

[2] Tanida J, Kumagai T, et al. "Thin Observation Module by Bound Optics (TOMBO): Concept and Experimental Verification.". Applied optics 40.11(2001): 1806-13.

[3] Jun Tanida, Hiroki Mima, Keiichiro Kagawa, Chizuko Ogata, Makoto Umeda, et al. "Application of a compound imaging system to odontotherapy". Optical Review 22.2(2015): 322-328.

[4] Luke P. Lee and Robert Szema. "Inspirations from Biological Optics for Advanced Photonic Systems". Science 310.5751(2005): 1148-1150.

[5] Ki-Hun Jeong and Jaeyoun Kim and Luke P. Lee. "Biologically Inspired Artificial Compound Eyes". Science 312.5773(2006): 557-561.

[6] Song Y M, Xie Y, Malyarchuk V, et al. "Digital cameras with designs inspired by the arthropod eye". Nature: International weekly journal of science 497.7447(2013): 95-99.

[7] Floreano D, Pericet-Camara R , Viollet, Stéphane, et al. "Miniature curved artificial compound eyes". Proceedings of the National Academy of Sciences 110.23(2013): 9267-9272.

[8] Richard Hornsey et al. "Electronic compound-eye image sensor: construction and calibration". IS&T/SPIE Electronic Imaging. pp. 13-24.

[9] R Krishnasamy, W Wong, E Shen, S Pepic, PJ Thomas. "High precision target tracking with a compound-eye image sensor." Conference on Electrical & Computer Engineering IEEE, 2004.

[10] Hongxia Zhang, Chenggang Zou, Le Song, Xiaodong Zhang, et al. "Curved compound eye imaging system with a large field of view based on a plano-concave substrate". Other Conferences. pp. 841805-841805-6.

[11] C Shi, Y Wang, C Liu, T Wang, W Yu. "SCECam: a spherical compound eye camera for fast location and recognition of objects at a large field of view." Optics Express 25.26(2017):32333.

[12] D. J. Brady et al. "Multiscale gigapixel photography". Nature: International weekly journal of science 486.7403(2012): 386-389.

[13] Axiu Cao et al. "Design and fabrication of a multifocal bionic compound eye for imaging". Bioinspiration & Biomimetics 13.2(2018).